〈일반논문〉
Journal of the Korean Society of Visualization, Vol. 20, No. 3 (19~26), 2022
(Manuscript received : 2022.10.16./Revised : 2022.10.26./Accepted : 2022.10.27.)
DOI:http://dx.doi.org/10.5407/jksv.2022.20.3.019

ISSN 1598-8430 Print
ISSN 2093-808X Online

표면파 유도 음향방사력을 이용한 미세액적의 크기 선별

무스타크 알리[*] · 차범석[*] · 무하마드 소반 칸[*] · 전현우[*] · 이송하[*] · 김우혁[*] · 고정우[*] · 박진수[†]

Size-based separation of microscale droplets by surface acoustic wave-induced acoustic radiation force

Mushtaq Ali[*], Beomseok Cha[*], Muhammad Soban Khan[*], Hyunwoo Jeon[*], Song Ha Lee[*], Woohyuk Kim[*], Jeongu Ko[*] and Jinsoo Park[†]

Abstract In droplet microfluidics, precise droplet manipulation is required in numerous applications. This study presents ultrasonic surface acoustic wave (USAW)-based microfluidic device for label-free droplet separation based on size. The proposed device is composed of a slanted-finger interdigital transducer on a piezoelectric substrate and a polydimethylsiloxane microchannel placed on the substrate. The microchannel is aligned in the cross-type configuration where the USAWs propagate in a perpendicular direction to the flow in the microchannel. When droplets are exposed to an acoustic field, they experience the USAW-induced acoustic radiation force (ARF), whose magnitude varies depending on the droplet size. We modeled the USAW-induced ARF based on ray acoustics and conducted a series of experiments to separate different-sized droplets. We found that the experimental results were in good agreement with the theoretical estimation. We believe that the proposed method will serve as a promising tool for size-based droplet separation in a label-free manner.

Key Words : Surface Acoustic Wave (표면파), Acoustofluidics (음향미세유체역학), Acoustic Radiation Force (음향방사력), Microscale Droplet (미세액적)

1. Introduction

In recent times, the capability of handling biological and chemical samples fundamentally in a new way using droplet microfluidics platform peaked the interest of the scientific society. Such a platform, where droplets are usually dispersed into another immiscible liquid, is broadly used in medical science such as drug delivery(1), biological assays(2), and cell encapsulation.(3) The rising popularity of droplet microfluidics is due to its increased throughput as it outputs thousands of droplets per second and the facilitation of contamination-free environment for a sensitive living cell. Increased profitability is guaranteed in droplet-based microfluidics by reducing the cost and time for a complex biological process by

[†] Department of Mechanical Engineering, Chonnam National University, Republic of Korea
Assistant Professor
E-mail: jinsoopark@jnu.ac.kr
[*] Department of Mechanical Engineering, Chonnam National University, Republic of Korea
Graduate Student

utilizing droplets of nanoliter to the picolitre scale.

The separation of droplets has great importance in the field of droplet microfluidics. The droplet separation phenomena are fundamentally associated with the selected markers for instance, size, shape, mass, density, and other intrinsic properties. Typically, the preliminary step is to detect based on aforementioned parameters which provides indications to move droplets differently. Many passive and active approaches have been reported for the separation of droplets. In inertial microfluidic platform, there exists many established techniques for droplet separation. Deterministic lateral displacement[4] practice is the oldest and a recognized technique used in this category. Pinched flow fractionation[5] is another widely used passive technique used in this sphere which uses laminar-flow focusing for size-dependent droplet sorting. Recently, Chang *et al.*[6] introduced a deformation-based droplet separation technique based on physical parameters such as viscosity, speed, and droplet size. Furthermore, Li *et al.*[7] produced hydrogel droplets using inertial equilibrium positions within microchannel and separated based on size. Certain limitations such as on-demand droplet separation, the formation of aerosols as a by-product, and necessity of specially designed microchannel geometry makes these approaches less versatile [8]. On the other hand, active approaches proposed by dielectrophoresis,[9] optophoresis,[10] magnetophoresis,[11] acoustophoresis[12], and thermocapillary[13] offer more advanced and efficient sorting. Among these, the acoustophoresis techniques, in which the force is induced by acoustic waves, provides an accurate and precise facilities for controlling microdroplets. Nevertheless, the existing active techniques still face challenges to separate droplets in continuous, simultaneous, and detection-free manner.

In this research, we designed an acoustofluidic device capable to manipulates droplets in a continuous, detection-free, and label-free manner. By incorporating the different magnitude of forces on the droplets due to differences in diameter, we can separate droplets precisely into the respective outlets to achieve size-based sorting and separation operations. Using a simple T-junction upstream, we first investigated the phenomena by producing water-in-oil droplets of multiple sizes and achieved sorting operation. We performed and analyzed experiments with varying acoustic power while maintaining the same droplet speed to keep flow-induced drag force constant. The effects of varying acoustic power were investigated by measuring the droplet retention distances. Based on the droplet sorting results, we achieved separation of two droplets possessing different diameter. We produced two different sized droplets alternately using double T-junction by simply adjusting the flow rate of continuous phase and dispersed phases. A cross-type microfluidic chip is used, having a slanted finger interdigital transducer (SFIT) on a piezoelectric substrate such that ultrasonic surface acoustic wave (USAW) is applied perpendicular to the flow direction. USAW-induced acoustic radiation force was analyzed using the ray acoustics approach. With these results, the proposed device shows excellent potential for fast, precise, continuous, and label-free droplet manipulation and can be utilized for drug screening and pharmaceuticals.

2. Methodology

Fig. 1(a) shows a perspective-view schematic diagram of the cross-type acoustofluidic device used in this research. The device is composed of SFIT which is deposited on lithium niobate (LN) substrate and polydimethylsiloxane (PDMS) microchannel. The SFIT which is comprised of Cr (30 nm) and Au (100 nm) was deposited on a 500 μm thick, 128° Y-cut, X-propagating LN substrate (MTI Korea). The electrode spacing of SFIT used in this study

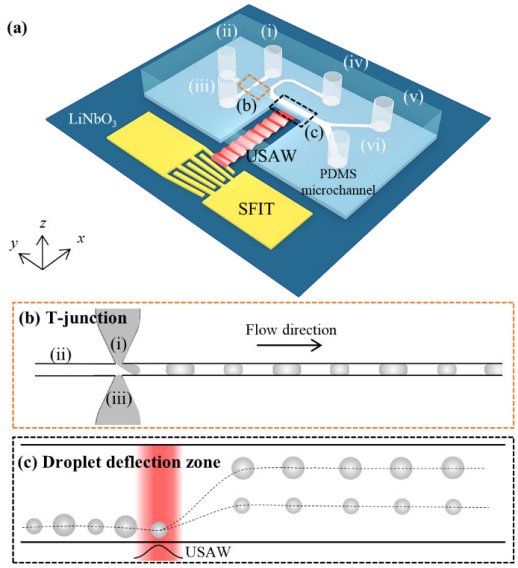

Fig. 1. (a) A perspective-view of a proposed cross-type acoustofluidic device used in this research. (b) generation of alternating droplet of different sizes at double T-junction. (c) behavior of droplets of varied sizes when they are exposed to ARF.

was 7 to 9 μm having their corresponding working frequency of 110 to 138 MHz. Using SFIT, ultrasonics traveling surface acoustic waves were produced on the LN substrate by inverse piezoelectric effect. The Gaussian-profile acoustic waves were produced from a transducer with the effective wave aperture of approximately 101.26 μm. Acoustofluidic devices are subject to the undesirable heating effect when the electrical power is applied to inefficiently designed transducers. In the proposed device, the electric power was as low as below 0.2 W. In addition, the SAW-based acoustofluidic devices have been widely used for biomedical applications where the temperature control is highly required and found to be biocompatible with high viability of the biological samples. [14] The PDMS microchannel was made through photolithography and soft lithography. After that it was bonded permanently onto the substrate through oxygen plasma bonding (Covance, Femto Science). The microchannel has three inlets which includes two dispersed phases (i and iii) and one continuous phase (ii), an additional inlet for sheath flow (iv) and two outlets (v and vi). The width of both continuous and dispersed phase channels was 30 μm whereas the height of microchannel was 180 μm. The width of droplet deflection zone was 500 μm where trajectories of multiple droplets were examined by measuring their retention distances. Retention distance is defined as the droplet migration distance due to the ultrasonic surface acoustic wave (USAW)-induced acoustic radiation force (ARF) with respect to the droplet trajectories without the acoustic field. The bonded microchannel was coated with fluorocarbon liquid (EGC-1720, 3M) prior to performing the experiments. A fluorocarbon oil (HFE-7500, 3M) was used as continuous phase fluid and DI water was used to as disperse phase fluid to produce droplets. Fluids were injected into the microchannels using a high-precision multi-unit syringe pump (neMESYS Cetoni GmbH). In order to create stable droplet interface 1 wt% of a nonionic surfactant (Pico-Surf™ 1, Dolomite Microfluidics, UK) in the continuous-phase fluid was added. To produce droplets of different size, flowrates of inlets were adjusted. Fig. 1(b) shows the production of two different-sized droplets at a double T-junction flowing from left to right. When exposed to acoustic radiation force, droplets behaved differently depending on the size, as shown in Fig. 1(c). In the case of microparticle manipulation using USAW induced ARF, asymmetric wave scattering off the solid elastic microsphere occurred in the Mie scattering regime [15]. On the contrary, the current work on the droplet sorting is based on the SAW-induced ARF derived from the asymmetric wave scattering off the fluid microsphere composed of two immiscible liquids occurred in the geometrical scattering regime. The two types of the ARFs are totally different in the working principle. We have previously proposed the elastic microsphere theory

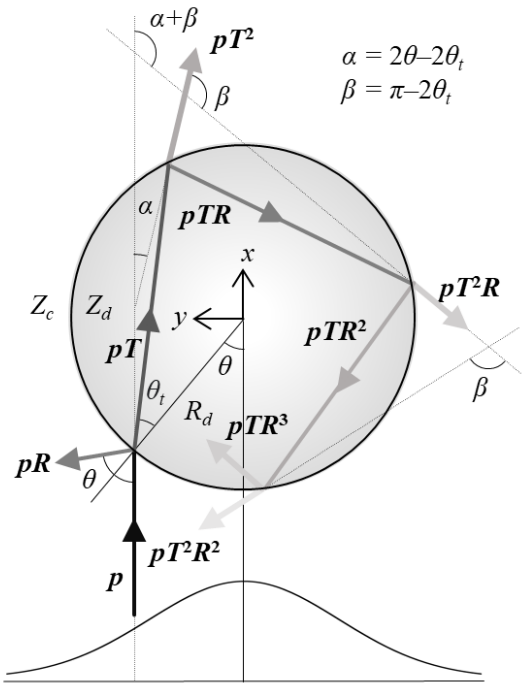

Fig. 2. 2D schematic diagram of the sphere located in the way of Gaussian shaped surface acoustic wave. It encountered a phonon ray which is then disintegrated into individual rays when hit to the droplet's surface.

to investigate the SAW-induced ARF on the solid spheres [16] whereas the current study proposes a ray acoustics model to estimate the SAW-induced ARF acting on the fluid spheres (droplets).

In the ray acoustic method, the incident beam is disintegrated into separate rays, each bringing a specific momentum ascertained by its intensity, direction, and transmission, as shown in Fig. 2. A beam carrying momentum (p) hits the droplets at an angle where it experiences partial reflection and transmission, giving rise to the moment transfer to the droplets, and the total force on the droplet is determined by the sum of the contribution of each ray. The ray change its path because of difference in acoustic impedances of water (Z_d) and the surrounding fluid (Z_c). The force obtained from this model, called acoustic radiation force, is dependent on the size of the droplet, acoustic wave intensity, wave reflection, and transmissions. Two components of ARF are the scattering component and the gradient component. The acoustic scattering component, which is directed in the direction of wave propagation, results from wave reflection, whereas the gradient component, which acts perpendicular to the wave propagation direction, is the result of wave transmission. Below is the expression of scattering component (F_s) of ARF:

$$F_s = \frac{1}{c_c}\int_0^{2\pi}\int_0^{\pi/2} I(D_d,\theta,\varphi) Q_x R_d^2 \sin(2\theta)\, d\theta\, d\varphi \qquad (1)$$

$$Q_x = 1 + R\cos(2\theta) - \frac{T^2\cos(2\theta - 2\theta_t) + R\cos(2\theta)}{1 + R^2 + 2R\cos(\theta_t)} \qquad (2)$$

where c_c represents the speed of sound in the continuous phase fluid, R_d is the radius of the droplet, φ is the polar angle, I is the acoustic intensity, θ and θ_t are the incident and refraction angles, respectively, and R and T are Fresnel reflection and transmission coefficients, respectively. Fig. 3 shows the numerically calculated results using

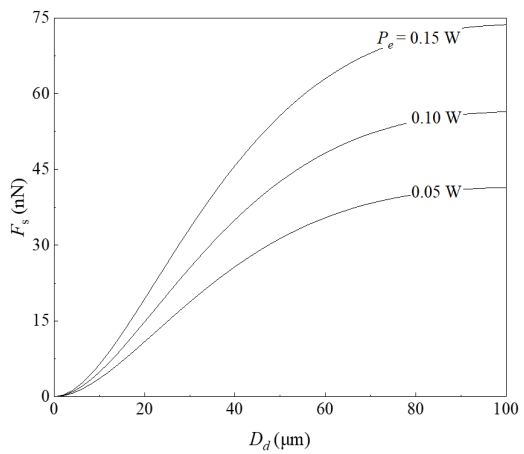

Fig. 3. Numerically calculated results using the ray acoustic approach for spherical droplets. The scattering components of acoustic radiation force (F_s) were plotted as a function droplet diameter (D_d).

the ray acoustic approach for spherical droplets at three acoustic powers (0.05 W 0.10 W and 0.15W. When the scattering components of acoustic radiation force (F_s) were plotted as a function droplet diameter (D_d), it can be seen that the magnitude of ARF increases with increasing droplet volume. This is witnessed because acoustic wave reflection dominates over refraction. Another countering force acting on the droplets while they are moving in the flow is the flow-induced drag force. In our experiments, we assumed to have a much smaller magnitude of drag force since we produced much smaller droplets compared to the microchannel height.

3. Results and Discussion

3.1 Sorting

To investigate the ARF effect on the droplet with varying sizes, we produced multiple-sized droplets using a simple T-junction upstream and recorded the deflection at a fixed acoustic power, as depicted in Fig. 4. We produced water-in-oil droplets having a diameter (D_d) much smaller than the height (h). Since $D_d << h$, the flow-induced drag force in a confined microchannel is much lowered. The size of the droplets could be easily controlled by altering volumetric flow rates of disperse phase and continuous phase fluids. Flowrates were tuned in such a way that droplet speeds were kept constant at approximately 12 mm/s for all trials in order to compare the results more effectively. Fig. 4(a) shows different droplet trajectories at D_d = 70–95 μm under the 120 MHz USAW applications with the fixed acoustic power (P_e = 0.05 W). As the D_d value increased from 70, 75, 80, 85, 90 to 95 μm, the droplet retention distance (d_R) was measured to increase from 142.11, 150.66, 176.27, 196.07, 202.88 to 221.57 μm, respectively. This is because surface area exposure to surface acoustic waves increases, thereby increasing wave reflection, leading to the increased magnitude of ARF. The retention distances for all the results showed an upward trend for increasing droplet diameter values, thereby validating the hypothesis based on the ray acoustic approach.

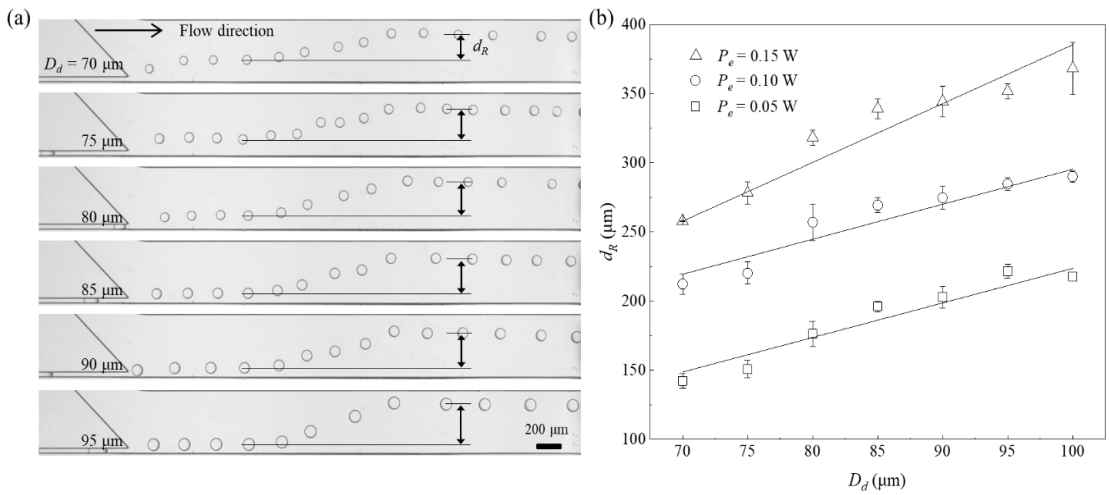

Fig. 4. (a) Experimental stacked microscopy images of size–based sorting of droplets with varying retention distance at P_e = 0.05 W. The deflection of droplets having a larger D_d is greater than that of droplets having a smaller D_d; (b) Experimental result of size-based sorting is plotted. The retention distance versus the droplet diameter. Higher value of D_d leads to the higher dR.

The intensity of wave amplitude was further increased, and the trajectories of the droplets were observed, taking the onset of acoustic radiation force as an origin. The droplets were characterized at three different values of acoustic power (0.05 W, 0.10 W and 0.15 W). A linear trend was noticed for all three USAW amplitudes when retention distance was plotted against the droplet diameter, as shown in Fig. 4(b). When acoustic power is increased by amplifying the voltage across the terminals of SFIT, the magnitude of incident rays is supposed to increase, thereby increasing ARF. Each data point represents the average of five experiments, and the error bars represent the standard deviation from the mean values.

3.2 Separation

After investigating the effect of ARF on various sizes of droplets in droplet sorting experiments, we finally performed the separation of two different-sized droplets simultaneously. Using a double T-junction upstream, we produced two different-sized droplets sequentially by simply adjusting the flow rate of the continuous phase and dispersed phases. The flow rates were adjusted, producing two droplets alternately, such that the diameter of the larger droplet (D_L) was 90 μm and the smaller droplet has diameter (D_S) was 75 μm. An additional inlet for sheath fluid was useful to maintain the distance between consecutive droplets, avoiding droplet-droplet interaction in the droplet deflection zone. In addition, droplet speed can easily be controlled by adjusting the flow rate of sheath fluid. Fig. 5 shows the experimental stacked microscopy images of two droplets of different sizes moving alternatively. Without the exposure of ARF, droplets were moving toward the below outlet without any deflection (Fig. 5(a)). But these continuously moving droplets witnessed significant retention distance when they experienced acoustic power of P_e = 0.024 W in the droplet deflection

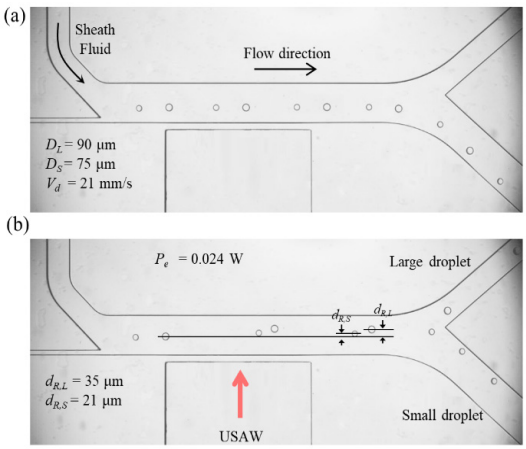

Fig. 5. Stacked microscopy images of size-based separation. (a) Without USAW, droplets moved toward the outlet undeflected. (b) After application of acoustic power (P_e = 0.024 W), large droplets and small droplets moved differently.

zone as shown in Fig. 5 (b). The large droplet shows substantial retention distance ($d_{R,L}$ = 35 μm) as compared to smaller droplet ($d_{R,S}$ = 21 μm). The retention distance difference between the two droplet was significant enough to move droplets into different outlets. The droplet speed in these experiments were measure as 21 mm/s.

4. Conclusion

In this study, we developed a cross-type acoustofluidic device capable of detection-free and continuous droplet separation based on size. We first achieved sorting operation by producing different sized droplets aiming to investigate the phenomena of ARF. Based on the findings, we successfully achieved separation of two different sized droplets simultaneously. In this device, acoustic waves were applied perpendicular to flow direction. The mechanism of acoustic radiation forces was analyzed using the ray acoustics approach. The acoustofluidic device proposed in the present study

may serve as a promising next-generation tool in droplet microfluidics for size-based separation without needing any labels. Moreover, for an appropriate assessment, we maintained the velocity of droplets to keep the flow-induced drag force constant. The effect of speed on droplet retention distance and drag force needs to be further investigated and explained in the future.

Acknowledgements

This work was financially supported by Chonnam National University (Grant number: 2021-2225) and the National Research Foundation of Korea (NRF) grant funded by the Korea government (MSIT) (No. 2020R1F1A1048611). The microfluidic devices were fabricated by using a mask aligner (MDA-400S, MIDAS) at Energy Convergence Core Facility in Chonnam National University.

REFERENCE

1) Demello, Andrew J. "Control and detection of chemical reactions in microfluidic systems." *Nature* 442, no. 7101 (2006): 394-402.
2) Theberge, Ashleigh B., Fabienne Courtois, Yolanda Schaerli, Martin Fischlechner, Chris Abell, Florian Hollfelder, and Wilhelm TS Huck. "Microdroplets in microfluidics: an evolving platform for discoveries in chemistry and biology." *Angewandte Chemie International Edition* 49, no. 34 (2010): 5846-5868.
3) Griffin, Donald R., Westbrook M. Weaver, Philip O. Scumpia, Dino Di Carlo, and Tatiana Segura. "Accelerated wound healing by injectable microporous gel scaffolds assembled from annealed building blocks." *Nature materials* 14, no. 7 (2015): 737-744.
4) Hochstetter, Axel, Rohan Vernekar, Robert H. Austin, Holger Becker, Jason P. Beech, Dmitry A. Fedosov, Gerhard Gompper et al. "Deterministic lateral displacement: Challenges and perspectives." *ACS nano* 14, no. 9 (2020): 10784-10795.
5) Maenaka, Hirosuke, Masumi Yamada, Masahiro Yasuda, and Minoru Seki. "Continuous and size-dependent sorting of emulsion droplets using hydrodynamics in pinched microchannels." *Langmuir* 24, no. 8 (2008): 4405-4410.
6) Chang, Yunju, Xinye Chen, Yuting Zhou, and Jiandi Wan. "Deformation-based droplet separation in microfluidics." *Industrial & Engineering Chemistry Research* 59, no. 9 (2019): 3916-3921.
7) Li, Ming, Mark van Zee, Keisuke Goda, and Dino Di Carlo. "Size-based sorting of hydrogel droplets using inertial microfluidics." *Lab on a Chip* 18, no. 17 (2018): 2575-2582.
8) Lee, Changyang, Jungwoo Lee, Hyung Ham Kim, Shia-Yen Teh, Abraham Lee, In-Young Chung, Jae Yeong Park, and K. Kirk Shung. "Microfluidic droplet sorting with a high frequency ultrasound beam." *Lab on a Chip* 12, no. 15 (2012): 2736-2742.
9) Zhao, Kai, and Dongqing Li. "Direct current dielectrophoretic manipulation of the ionic liquid droplets in water." *Journal of Chromatography A* 1558 (2018): 96-106.
10) Jung, Jin Ho, Kyung Heon Lee, Kang Soo Lee, Byung Hang Ha, Yong Suk Oh, and Hyung Jin Sung. "Optical separation of droplets on a microfluidic platform." *Microfluidics and nanofluidics* 16, no. 4 (2014): 635-644.
11) Zhang, Kai, Qionglin Liang, Sai Ma, Xuan Mu, Ping Hu, Yiming Wang, and Guoan Luo. "On-chip manipulation of continuous picoliter-volume superparamagnetic droplets using a magnetic force." *Lab on a Chip* 9, no. 20 (2009): 2992-2999.
12) Li, Sixing, Xiaoyun Ding, Feng Guo, Yuchao Chen, Michael Ian Lapsley, Sz-Chin Steven Lin, Lin Wang, J. Philip McCoy, Craig E. Cameron, and Tony Jun Huang. "An on-chip, multichannel droplet sorter using standing surface acoustic waves." *Analytical chemistry* 85, no. 11 (2013):

5468-5474.

13) Robert de Saint Vincent, Matthieu, Régis Wunenburger, and Jean-Pierre Delville. "Laser switching and sorting for high speed digital microfluidics." *Applied Physics Letters* 92, no. 15 (2008): 154105.

14) Wiklund, Martin. "Acoustofluidics 12: Biocompatibility and cell viability in microfluidic acoustic resonators." *Lab on a Chip* 12, no. 11 (2012): 2018-2028.

15) Ahmad, Raheel, Ghulam Destgeer, Muhammad Afzal, Jinsoo Park, Husnain Ahmed, Jin Ho Jung, Kwangseok Park, Tae-Sung Yoon, and Hyung Jin Sung. "Acoustic wave-driven functionalized particles for aptamer-based target biomolecule separation." *Analytical chemistry* 89, no. 24 (2017): 13313-13319..

16) Destgeer, Ghulam, Byung Hang Ha, Jinsoo Park, Jin Ho Jung, Anas Alazzam, and Hyung Jin Sung. "Microchannel anechoic corner for size-selective separation and medium exchange via traveling surface acoustic waves." *Analytical chemistry* 87, no. 9 (2015): 4627-4632.